eprints@whiterose.ac.uk
https://eprints.whiterose.ac.uk/

White Noise Reduction for Wideband Beamforming Based on Uniform Rectangular Arrays

Mohammad Reza Anbiyaei and Wei Liu
Department of Electronic and Electrical Engineering
University of Sheffield
Sheffield S1 3JD, UK

Des C. McLernon
School of Electronic and Electrical Engineering
University of Leeds
Leeds LS2 9JT, UK

Abstract—**Two methods are proposed for reducing the effect of white noise in wideband uniform rectangular arrays via a combination of judiciously designed transformations followed by a series of highpass filters. The reduced noise level leads to a higher signal to noise ratio for the system, which in turn results in a clear improvement on the performance of various beamforming applications. As a representative example, the reference signal based (RSB) and the linearly constrained minimum variance (LCMV) beamformers are employed here to demonstrate the improved performance, which is also confirmed by simulations.**

I. INTRODUCTION

Wideband beamfomring has been an active field of research for many years and has a wide range of applications including radar, sonar and wireless communications [1], [2], [3].

In general, the performance of all wideband beamforming algorithms is dependent on the level of noise in the system, and normally the lower the level of noise, the better is the performance. In most cases, noise in wideband arrays is spatially (and also temporally in many cases) white, i.e., the noise at each array sensor is uncorrelated with the noise at any other sensor. It seems that there is not much that can be done about the noise and we have to simply accept whatever noise is left after processing for the signal component.

In our previous work [4], a method was developed for reducing the effect of white noise in wideband uniform linear arrays (ULAs) via a combination of a judiciously designed transformation followed by highpass filters to improve the performance for wideband direction of arrival (DOA) estimation. Here we extend this idea to the case of uniform rectangular arrays (URAs) [5], [6], [7]. As a result, the transformation matrix has to be re-designed to adjust the noise reduction method to the structure of URAs.

In particular, two noise reduction methods are introduced in this paper for URAs and for each one, a different transformation is designed. The first method is based on a two-dimensional (2D) transformation. The second method is an adaptation of our previous work for ULAs [4], which is based on one-dimensional (1D) transformation of the signals received by the URA. The transformations must be invertible and ideally, unitary. As representative examples for unitary transformations, 2D-DFT (discrete Fourier transform) and 1D-DFT are used in simulations.

Both methods can increase the overall signal to noise ratio (SNR) of the array. This improvement leads to performance enhancement of various array signal processing applications such as beamforming, which is demonstrated by simulations using two well-known adaptive beamformers, namely the reference signal based (RSB) [8], [9], [10], [11], and the linearly constrained minimum variance (LCMV) beamformers [3], [12].
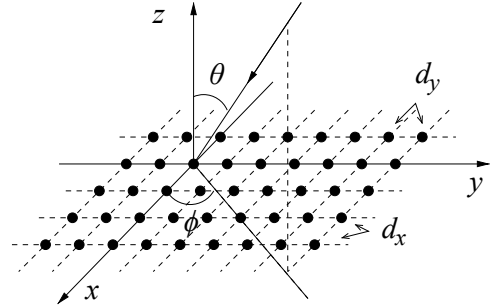

Fig. 1: The structure of a URA, where a signal impinges from azimuth angle θ and elevation angle ϕ .

This paper is organised as follows. In Sec. II, the proposed white noise reduction method for URAs with a 2D transformation is introduced. In Sec. III, the proposed white noise reduction method for URAs with a 1D transformation is explained. Simulation results are presented in Sec. IV, followed by conclusions in Sec. V.

II. THE PROPOSED WHITE NOISE REDUCTION METHOD FOR URAS WITH A 2D TRANSFORMATION

The structure of a URA is shown in Fig. 1, and a block diagram for the general structure of the proposed noise reduction method is shown in Fig. 2. Suppose there are M sensors along the x-axis and N sensors along the y-axis. The received array signals $x_{m,l}[n]$, $m = 0, \ldots, M - 1$, $l = 0, \ldots, N - 1$, are first transformed by a 2D transformation and then its outputs $q_{m,l}[n], m = 0, \cdots, M - 1$, $l = 0, \cdots, N - 1$, pass through a set of highpass filters with impulse responses given by $h_{m,l}[n], m = 0, \cdots, M - 1, l = 0, \cdots, N - 1$. The outputs of the highpass filters $z_{m,l}, m = 0, \cdots, M-1, l = 0, \cdots, N-1$, are then transformed by the inverse of the 2D transformation.

There are two components for the received array signal $x_{m,l}[n]$ at the (m, l)-th sensor: the directional signal part $s_{m,l}[n]$ and the white noise part $\bar{n}_{m,l}[n]$, i.e.,

$$x_{m,l}[n] = s_{m,l}[n] + \bar{n}_{m,l}[n]. \tag{1}$$

The complete $M \times N$ signal matrix $\mathbf{X}[n]$ can be expressed as

$$\mathbf{X}[n] = \mathbf{S}[n] + \bar{\mathbf{N}}[n], \tag{2}$$

where

$$\mathbf{X}[n] = [\mathbf{x}_0[n], \mathbf{x}_1[n], \cdots, \mathbf{x}_{N-1}[n]],$$

$$\mathbf{S}[n] = [\mathbf{s}_0[n], \mathbf{s}_1[n], \cdots, \mathbf{s}_{N-1}[n]],$$

$$\bar{\mathbf{N}}[n] = [\bar{\mathbf{n}}_0[n], \bar{\mathbf{n}}_1[n], \cdots, \bar{\mathbf{n}}_{N-1}[n]].$$
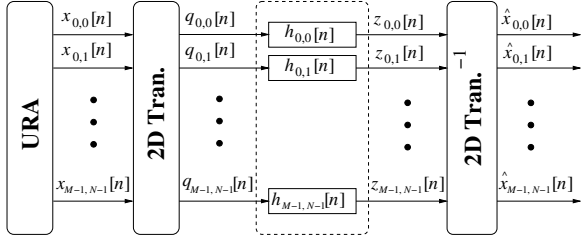
Fig. 2: A block diagram of the proposed noise reduction method based on a 2D transformation.

Fig. 3: Frequency responses of the 2D transformation applied to an $M \times N$ URA.

and

$$\mathbf{x}_l[n] = [x_{0,l}[n], x_{1,l}[n], \cdots, x_{M-1,l}[n]]^T,$$

$$\mathbf{s}_l[n] = [s_{0,l}[n], s_{1,l}[n], \cdots, s_{M-1,l}[n]]^T,$$

$$\bar{\mathbf{n}}_l[n] = [\bar{n}_{0,l}[n], \bar{n}_{1,l}[n], \cdots, \bar{n}_{M-1,l}[n]]^T,$$

with $l = 0, 1, \cdots, N-1$.

In this method, we transform the array signal $\mathbf{X}[n]$, which is received by an $M \times N$ URA, with a 2D unitary transformation. The output matrix $\mathbf{Q}[n]$ of the transformation is [13], [14],

$$\mathbf{Q}[n] = \mathbf{A}\mathbf{X}[n]\mathbf{B}, \tag{3}$$

where $\mathbf{A}$ and $\mathbf{B}$ are $M \times M$ and $N \times N$ transform matrices, respectively, and they are assumed to be unitary and together form the 2D transformation.

The element of $\mathbf{A}$ at the m-th row and i-th column is denoted by $a_{m,i}$, i.e., $[\mathbf{A}]_{m,i} = a_{m,i}$, and the element of $\mathbf{B}$ at the k-th row and l-th column is denoted by $b_{k,l}$, i.e., $[\mathbf{B}]_{k,l} = b_{k,l}$. Each pair of a row vector of $\mathbf{A}$ and a column vector of $\mathbf{B}$ acts as a simple beamformer, and its output $q_{m,l}$ is given by

$$q_{m,l}[n] = \sum_{i=0}^{M-1} \sum_{k=0}^{N-1} a_{m,i} b_{k,l} x_{i,k}[n]. \tag{4}$$

The beam response $R_{m,l}(\Omega, \theta, \phi)$ of this beamformer as a function of the normalized frequency Ω, azimuth angle θ and elevation angle ϕ is

$$R_{m,l}(\Omega, \theta, \phi) = \sum_{i=0}^{M-1} \sum_{k=0}^{N-1} a_{m,i} b_{k,l} e^{-j\Omega \sin\theta(i\mu_x \cos\phi + k\mu_y \sin\phi)}, \tag{5}$$

where $\mu_x = \frac{d_x}{cT_s}$, $\mu_y = \frac{d_y}{cT_s}$ and $\Omega = \omega T_s$, with c being the wave propagation speed, T_s the sampling period, $j = \sqrt{-1}$, d_x and d_y the array spacings along the x-axis and y-axis, and ω the angular frequency of signals.

With $\Omega_1 = \mu_x \Omega \sin\theta \cos\phi$ and $\Omega_2 = \mu_y \Omega \sin\theta \sin\phi$, we have:

$$A_{m,l}(\Omega_1, \Omega_2) = \sum_{i=0}^{M-1} \sum_{k=0}^{N-1} a_{m,i} b_{k,l} e^{-ji\Omega_1 - jk\Omega_2}, \tag{6}$$

where $A_{m,l}(\Omega_1, \Omega_2)$ is the frequency response of the pair of m-th row vector of the transformation matrix $\mathbf{A}$ and the l-th column vector of the transformation $\mathbf{B}$, considering each row vector and column vector pair as defining the impulse response of a separable 2D finite impulse response (FIR) filter.
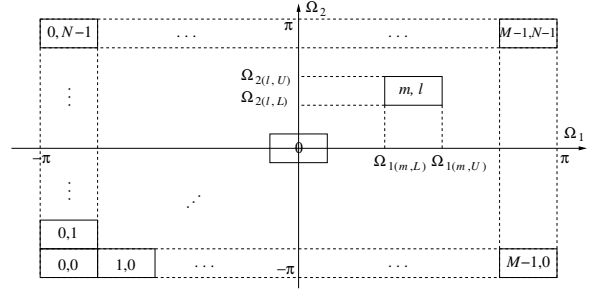
Equation (6) can be rearranged as

$$\sum_{i=0}^{M-1} a_{m,i} e^{-ji\Omega_1} \sum_{k=0}^{N-1} b_{k,l} e^{-jk\Omega_2} = A_m(\Omega_1) A_l(\Omega_2), \tag{7}$$

where $A_m(\Omega_1)$ is the frequency response of the m-th row vector of the transformation matrix $\mathbf{A}$ and $A_l(\Omega_2)$ is the frequency response of the l-th column vector of the transformation matrix $\mathbf{B}$. By substituting $\Omega_1 = \mu_x \Omega \sin\theta \cos\phi$ and $\Omega_2 = \mu_y \Omega \sin\theta \sin\phi$ in (7) and considering (5), we have

$$R_{m,l}(\Omega, \theta, \phi) = A_m(\mu_x \Omega \sin\theta \cos\phi) A_l(\mu_y \Omega \sin\theta \cos\phi). \tag{8}$$

So, the beam pattern of the (m,l)-th 2D transformation is the frequency response of the m-th row vector of $\mathbf{A}$ multiplied by frequency response of the l-th column vector of $\mathbf{B}$.

By assuming that the sampling frequency is twice the highest frequency component of the wideband signal and the array spacings (d_x, d_y) are half the wavelength of the highest frequency component, we have $\mu_x = \mu_y = 1$ [3]. The frequency responses $A_{m,l}(\Omega_1, \Omega_2), m = 0, \cdots, M-1, l = 0, \cdots, N-1$, are arranged to be bandpass, each with a bandwidth of $2\pi/M$ for Ω_1 and $2\pi/N$ for Ω_2 in the 2D frequency domain. The row vectors of $\mathbf{A}$ and column vectors of $\mathbf{B}$ all together cover the whole 2D frequency band, which is $\Omega_1, \Omega_2 \in [-\pi : \pi]$. An ideal example of the 2D bandpass filter responses in the 2D frequency domain is shown in Fig. 3.

The 2D bandpass filters have a highpass filtering effect on the received array signals. Taking the pair of m-th row vector of $\mathbf{A}$ and l-th column vector of $\mathbf{B}$ as an example, its frequency repsonse is

$$|A_{m,l}(\Omega_1, \Omega_2)| = \begin{cases} 1, & \text{for } \Omega_1 \in [\Omega_{1(m,L)}; \Omega_{1(m,U)}] \\ & \& \ \Omega_2 \in [\Omega_{2(l,L)}; \Omega_{2(l,U)}] \\ 0, & \text{otherwise.} \end{cases} \tag{9}$$

Considering the above frequency response, the received array signal components with frequency of $\Omega \in [-\Omega_{1(m,L)} : \Omega_{1(m,L)}]\&[-\Omega_{2(l,L)} : \Omega_{2(l,L)}]$ will not pass through this row vector, since $\Omega_1 = \Omega \sin\theta \cos\phi$ and $\Omega_2 = \Omega \sin\theta \sin\phi$ does not fall into the passband of $[\Omega_{1(m,L)} : \Omega_{1(m,U)}]$ and $[\Omega_{2(l,L)} : \Omega_{2(l,U)}]$, no matter what value the DOA angles (θ, ϕ) take. Therefore, the frequency range of the output is $|\Omega| \geq \min(\Omega_{1(m,L)}, \Omega_{2(l,L)})$ and the lower bound is determined by $\min(\Omega_{1(m,L)}, \Omega_{2(l,L)})$ when $\Omega_{1(m,L)}$ and $\Omega_{2(l,L)} \geq 0$. We need to consider the negative values for Ω_1 and Ω_2 as well. Therefore, more generally, the frequency range of the output is $|\Omega| \geq \min(|\Omega_{1(m,L)}|, |\Omega_{1(m,U)}|, |\Omega_{2(l,L)}|, |\Omega_{2(l,U)}|)$,
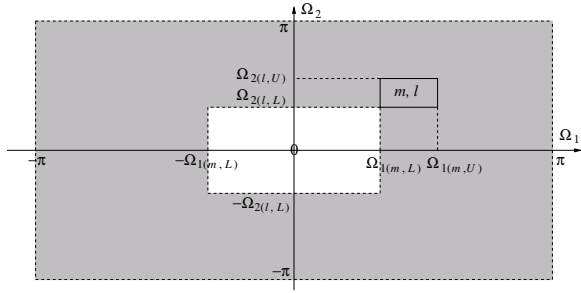
Fig. 4: The highpass filtering effect of the (m, l)-th 2D filter in the ideal case.
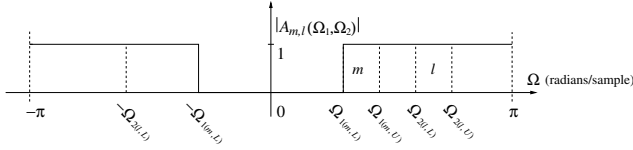

Fig. 5: The highpass filtering effect of the (m, l)-th 2D filter in the signal frequency domain in the ideal case.

with lower bound determined by $\min(|\Omega_{1(m,L)}|, |\Omega_{1(m,U)}|, |\Omega_{2(l,L)}|, |\Omega_{2(l,U)}|)$.

Therefore, the output spectrum of the directional signal part of $q_{m,l}[n]$ from (4) corresponding to the m-th row vector of $\mathbf{A}$ and the l-th column vector of $\mathbf{B}$ is highpass filtered as demonstrated in Fig. 4 in the 2D frequency domain, and its effect on the signal frequency domain is shown in Fig. 5. Since the noise part at the array sensors is spatially white, the output noise spectrum of each pair of transformation vectors is still a constant, covering the whole spectrum. Assuming the row vectors of $\mathbf{A}$ and the column vectors of $\mathbf{B}$ are normalized to unity norm, there would be no change to the total noise power after the transformation.

Each $q_{m,l}[n], m = 0, \cdots, M-1, l = 0, \cdots, N-1$, is the input to the corresponding highpass filter $h_{m,l}[n], m = 0, \cdots, M-1, l = 0, \cdots, N-1$, and that filter should cover the whole bandwidth of the signal part, i.e., having the same highpass frequency response as shown in Fig. 5. Therefore, ideally the highpass filters will not have any effect on the signal part and the signal part should pass through the highpass filters without any distortion. But the frequency components of the white noise which fall into the stopband of the highpass filters will in fact be removed. The output of these highpass filters is given by

$$\mathbf{Z}[n] = \begin{bmatrix} z_{0,0}[n] & \cdots & z_{0,N-1}[n] \\ \vdots & \ddots & \vdots \\ z_{M-1,0}[n] & \cdots & z_{M-1,N-1}[n] \end{bmatrix}, \quad (10)$$

where $z_{m,l}[n] = q_{m,l}[n] * h_{m,l}[n], m = 0, \cdots, M-1, l = 0, \cdots, N-1$, and $*$ denotes the convolution operator.

By applying the 2D inverse transformation to $\mathbf{Z}[n]$, we obtain the estimates of the original input sensor signals $\hat{x}_{m,l}[n], m = 0, \cdots, M-1, l = 0, \cdots, N-1$. In matrix form, we have:

$$\hat{\mathbf{X}}[n] = \mathbf{A}^{-1}\mathbf{Z}[n]\mathbf{B}^{-1}, \quad (11)$$

where $\mathbf{A}^{-1}$ and $\mathbf{B}^{-1}$ are the inverse of the corresponding transformation matrices. The original directional array signal

will be recovered without distortion in the ideal case, while the noise power will be reduced, leading to an improved total signal power to noise ratio (TSNR).

Considering the stopband of each highpass filter, the total effect of the highpass filters on the total noise power can be calculated. By using numeric methods, it has been calculated that when $M, N \to \infty$, the power of noise will be reduced by 1.76dB. Therefore, up to a maximum of 1.76dB improvement in TSNR can be achieved. However, in practice, the TSNR improvement will be less than that, due to the limited number of sensors in the URA. This TSNR improvement is less than the 3dB improvement which was achieved for ULAs using a 1D unitary transformation as in our previous work [4]. In the next section, as an alternative approach, we adapt the noise reduction method for ULAs to be applicable to URAs, in order to achieve a better output TSNR.

III. THE PROPOSED WHITE NOISE REDUCTION METHOD FOR URAS WITH A 1D TRANSFORMATION

In this approach, the method developed for ULAs in [4] is adapted for the new URA structure. Each column of the sensors of a URA is actually a ULA. Therefore, we take each column of the sensors separately as a ULA and apply the previously developed noise reduction method for the ULAs to each column. As a result, along each column of sensors we will have a 3dB improvement in the SNR of that column. Considering the whole URA structure, we achieve 3dB TSNR improvement. In the following, this approach is explained in more details.

Assume the l-th column of sensors along the x-axis, is considered for processing. $\mathbf{x}_l[n] = [x_{0,l}[n], x_{1,l}[n], \cdots, x_{M-1,l}[n]]^T$ is the signal vector according to this column. $\mathbf{x}_l[n]$ is transformed with a 1D transformation matrix such as $\mathbf{A}$, with size $M \times M$. After transforming $\mathbf{x}_l[n]$, we obtain the output signal vector $\mathbf{q}_l[n]$ as

$$\mathbf{q}_l[n] = \mathbf{A}\mathbf{x}_l[n], \quad (12)$$

where $\mathbf{q}_l[n] = [q_{0,l}[n], \cdots, q_{M-1,l}[n]]^T$.

The highpass filtering effect of the transformation for ULAs has been shown in [4]. Because of the highpass filtering effect of the transformation on the directional signal, the output spectrum of the directional signal part of $q_{m,l}[n]$ corresponding to the m-th row vector of $\mathbf{A}$ is highpass filtered. As the noise part of the array sensors is spatially white, the output noise spectrum of the row vector is still a constant, covering the whole spectrum. Since $\mathbf{A}$ is assumed to be unitary and the row vectors of $\mathbf{A}$ are normalized to unity norm, therefore, there would be no change to the total noise power after transformation.

Similar to the explanation for (10), each $q_{m,l}[n], m = 0, \cdots, M-1$, is the input to the corresponding highpass filter $h_{m,l}[n], m = 0, \cdots, M-1$, and the highpass filter should cover the whole bandwidth of the signal part, i.e., having the same highpass frequency response. Therefore, ideally the highpass filters will not have any effect on the signal part and the signal part should pass through the highpass filters without any distortion. However, frequency components of the white noise which fall into the stopband of the highpass filters will be removed. The output of these highpass filters is given by

$$\mathbf{z}_l[n] = \begin{bmatrix} z_{0,l}[n] \\ z_{1,l}[n] \\ \vdots \\ z_{M-1,l}[n] \end{bmatrix} = \begin{bmatrix} q_{0,l}[n] * h_{0,l}[n] \\ q_{1,l}[n] * h_{1,l}[n] \\ \vdots \\ q_{M-1,l}[n] * h_{M-1,l}[n] \end{bmatrix}. \quad (13)$$

Applying the inverse of the transformation matrix $(\mathbf{A}^{-1})$ to $\mathbf{z}_l[n]$, we obtain the estimates of the original input sensor signals $\hat{x}_{m,l}[n]$, $m = 0, \cdots, M - 1$. In vector form, we have

$$\hat{\mathbf{x}}_l[n] = \mathbf{A}^{-1}\mathbf{z}_l[n], \tag{14}$$

where $\hat{\mathbf{x}}_l[n] = [\hat{x}_{0,l}[n], \hat{x}_{1,l}[n], \cdots, \hat{x}_{M-1,l}[n]]^T$. After going through these processing stages, ideally, there is no change in the signal part in the final output $\hat{x}_{m,l}[n]$, $m = 0, \cdots, M - 1$, compared to the original signal part in $x_{m,l}[n]$, $m = 0, \cdots, M - 1$. However, since $\mathbf{A}^{-1}$ is also unitary, the total noise power stays the same between $\hat{\mathbf{x}}_l[n]$ and $\mathbf{z}_l[n]$. Following the same analysis for the ULA case as discussed in [4], we can draw the same conclusion that up to 3dB TSNR improvement can be obtained by the proposed method. However, in practice, the SNR improvement will be less than 3dB due to the limited number of sensors. The same process needs to be applied to all the columns of sensors of the URA across the x-axis, and for each column of sensors a 3dB improvement in TSNR will be achieved.

However, one important point is that, although the TSNR improvement is 3dB and much higher than the case of the 2D transformation developed in the last section, the sidelobe attenuation of the 1D case will be much less than the 2D case. Because as shown in (8), the beampattern of the 2D transformation is the multiplication of the beampatterns of its corresponding row/column vectors. A direct consequence will be more distortion to the signal part using the 1D transformation when discarding the noise components using the highpass filters. As a result, the performance improvement may be less than the method directly based on the 2D transformation. This will be demonstrated in the next section.

IV. SIMULATION RESULTS

In this section, simulation results will be provided and compared to verify the effectiveness of the two proposed noise reduction preprocessing methods for URAs. For simplicity the same number of sensors is used across the x-axis and y-axis ($M = N$), with the same array spacings ($d_x = d_y$). The URA has 16 sensors along each axis ($M = 16$) and the desired signal arrives from the broadside ($\theta_d, \phi_d = 0$). The transformation matrix $\mathbf{A} = \mathbf{B}$ is a 16×16 DFT matrix, as an example of unitary transformation. For the highpass filters, linear phase 50-tap FIR filters with a common delay of 25 samples are employed. Then, the array signals are transformed back by the inverse of the transformation matrix ($\mathbf{A}^{-1}$).

As mentioned before, by using the 2D transformation method, up to 1.76dB and by using the 1D transformation method, up to 3dB TSNR improvement can be achieved. Despite lower TSNR improvement, the 2D transformation method has less distortion on the directional signal, because the 2D transformation vectors have a higher sidelobe attenuation, due to the dual filtering process along both axes. Frequency responses of an example 2D-DFT vector in the frequency domain and its corresponding 1D-DFT vector, for the directional signal arriving from $\theta = 90°$ and $\phi = 45°$ are shown in Fig. 6. It can be clearly seen that the sidelobe attenuation for the 2D-DFT is around 26dB, whereas the sidelobe attenuation for the 1D-DFT is around 13dB. This results to less amount of directional signals available in the lower sidelobes of the 2D-DFT, to be removed by the highpass filters compared to the 1D-DFT. Therefore, we will have a better recovery for the directional signals after the inverse transformation. To compare the performance of the two methods in recovering
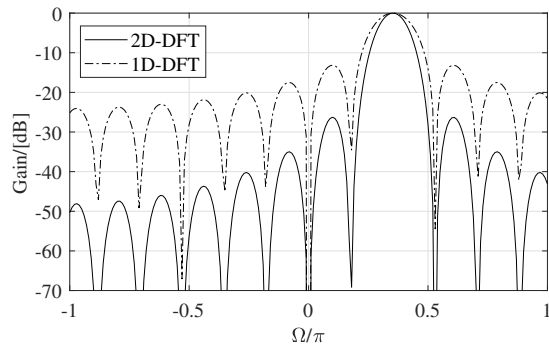

Fig. 6: Frequency responses of an example 2D-DFT vector and its corresponding 1D-DFT vector, for the directional signal arriving from $\theta = 90°$ and $\phi = 45°$.

the directional signal, wideband signals with unit power from random directions are applied to the URA, and then processed by the noise reduction methods. The mean square error (MSE) between the original signal and the recovered one by both methods is calculated for different URA sizes (M) with 10,000 Monte Carlo runs [15], and the results are presented in Table I. It is clear that the effect on the directional signal for the method using the 2D-DFT is much smaller compared to the method using the 1D-DFT, and hence better recovery.

Now we examine the effect of the two proposed methods on the performance of both the RSB beamformer and the LCMV beamformer. When the directional signal is arriving from the broadside, there is no delay between the received array signals. Therefore, most of the signal power appears in the output of the transformation covering the zero frequency, which is not affected by the corresponding highpass filter. This leads to an almost distortionless output for both methods. In the following simulations, the desired signal is first assumed to be arriving from the broadside. Otherwise, we can use pre-steering to change the look direction. When the desired signal is arriving from a direction other than broadside, both methods will have a small distortion on the desired signal. The method with a 1D-DFT has a higher SNR improvement, so for low input SNR values, it is expected that the beamformer will have a better SINR performance compared to the method with a 2D-DFT. On the other hand, when the input SNR is high enough, the 2D-DFT method should have a better performance, as it has less distortion on the desired signal. For very high SNR values, as the effect of noise is almost negligible, better beamforming performance is expected by not applying any noise reduction.

M	2D-DFT	1D-DFT
10	8.25×10^{-4}	2.04×10^{-2}
16	6.63×10^{-4}	1.85×10^{-2}
20	5.66×10^{-4}	1.75×10^{-2}
30	3.79×10^{-4}	1.43×10^{-2}
40	2.80×10^{-4}	1.20×10^{-2}

TABLE I: MSE for the directional signal before and after the proposed noise reduction process for different URA sizes.

First, we assume a desired bandlimited signal with bandwidth of $[0.3\pi, \pi]$ is received by the URA from the broadside. Seven interfering signals are applied to the system, each with a -10dB input SIR and their DOAs are $\theta_i = 10°$, $20°$, $30°$, $40°$, $50°$, $60°$ and $70°$, respectively, all with $\phi = 45°$. A
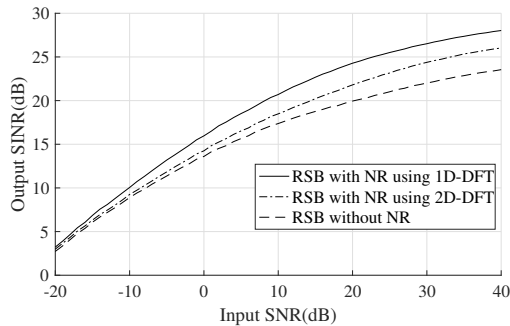
(a) RSB beamformer.
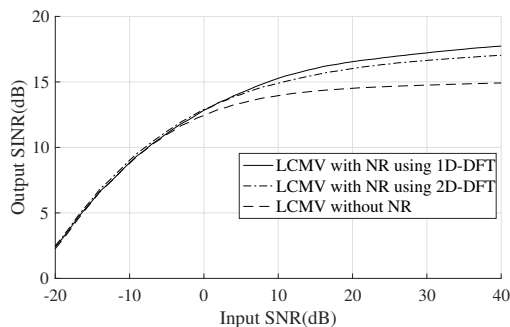
(b) LCMV beamformer.

Fig. 7: SINR performance of both beamformers with and without the proposed noise reduction (NR) methods for the URA.

Fig. 8: SINR performance of the RSB beamformer with the desired signal arriving from $\theta_d = 5°$ and $\phi_d = 0$.

tapped delay-line (TDL) length of $J = 30$ is used for these beamformers.

The results are shown in Fig. 7. A higher output SINR is achieved by both proposed noise reduction methods for both beamformers for all the input SNR range and generally the improvement becomes larger when the input SNR increases. As the SNR improvement of the noise reduction method with a 1D-DFT is higher than the SNR improvement of the method with a 2D-DFT, a higher SINR improvement is achieved for both beamformers using the method with a 1D-DFT.

At last, we have given an example to show the effect caused by the different distortions using the two different noise reduction methods. The SINR performance of the RSB beamformer is shown in Fig. 8, with the desired signal arriving from $\theta_d = 5°$ and $\phi_d = 0$, and other conditions are the same. As expected, for low SNR values, the performance is higher using a 1D-DFT noise reduction method. As the SNR increases the 2D-DFT method shows a better performance due to less distortion of the desired signal. For very high input SNR values better performance is achieved by not using any noise reduction method, since the effect of noise is almost negligible, while the distortion to the desired signal caused by the noise reduction methods becomes the dominant factor.

V. CONCLUSIONS

Two methods for mitigating the effect of white noise without affecting the directional signal in wideband URAs has been introduced. With the proposed method using a 2D transformation, a maximum of 1.76dB improvement in TSNR can be achieved in the ideal case, which is less than the 3dB improvement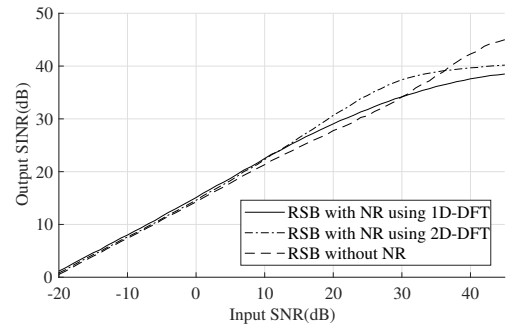 previously achieved for ULAs. As an alternative, the noise reduction method using a 1D transformation for the URAs is proposed, which is a direct adaptation of the method used for ULAs, with a 3dB improvement achieved. Despite lower improvement in TSNR, the 2D transformation method has less distortion for directional signals. The increased TSNR can be translated into performance improvement in various URA signal processing applications and as an example its effect on adaptive beamforming was studied. As demonstrated by simulation results, a clear improvement in performance in terms of output SINR has been achieved for a range of input SNR values.

REFERENCES

[1] H. L. Van Trees, *Optimum Array Processing, Part IV of Detection, Estimation, and Modulation Theory*, Wiley, New York, 2004.
[2] B. Allen and M. Ghavami, *Adaptive Array Systems, Fundamentals and Applications*, John Wiley & Sons, Chichester, England, 2005.
[3] W. Liu and S. Weiss, *Wideband Beamforming: Concepts and Techniques*, John Wiley & Sons, Chichester, UK, 2010.
[4] M. R. Anbiyaei, W. Liu, and D. C. McLernon, "Performance improvement for wideband DOA estimation with white noise reduction based on uniform linear arrays," in *Proc. IEEE, Sensor Array and Multichannel Signal Processing Workshop (SAM)*, Rio de Janeiro, Brazil, July 2016.
[5] M. Ghavami, "Wideband smart antenna theory using rectangular array structures," *IEEE Transactions on Signal Processing*, vol. 50, no. 9, pp. 2143–2151, September 2002.
[6] P. Ioannides and C. A. Balanis, "Uniform circular and rectangular arrays for adaptive beamforming applications," *IEEE Antennas and Wireless Propagation Letters*, vol. 4, no. 1, pp. 351–354, 2005.
[7] W. Liu, "Design and implementation of a rectangular frequency invariant beamformer with a full azimuth angle coverage," *Journal of the Franklin Institute*, vol. 348, pp. 2556–2569, November 2011.
[8] R. T. Compton, Jr., "The relationship between tapped delay-line and FFT processing in adaptive arrays," *IEEE Transactions on Antennas and Propagation*, vol. 36, no. 1, pp. 15–26, January 1988.
[9] R. T. Compton, "The bandwidth performance of a two-element adaptive array with tapped delay-line processing," *IEEE Transactions on Antennas and Propagation*, vol. 36, no. 1, pp. 4–14, January 1988.
[10] F. W. Vook and R. T. Compton, Jr., "Bandwidth performance of linear adaptive arrays with tapped delay-line processing," *IEEE Transactions on Aerospace and Electronic Systems*, vol. 28, no. 3, pp. 901–908, July 1992.
[11] N. Lin, W. Liu, and R. J. Langley, "Performance analysis of an adaptive broadband beamformer based on a two-element linear array with sensor delay-line processing," *Signal Processing*, vol. 90, pp. 269–281, January 2010.
[12] O. L. Frost, III, "An algorithm for linearly constrained adaptive array processing," *Proceedings of the IEEE*, vol. 60, no. 8, pp. 926–935, August 1972.
[13] A. K. Jain, *Fundamentals of digital image processing*, Prentice-Hall, Inc., 1989.
[14] J. S. Lim, *Two-dimensional signal and image processing*, Prentice-Hall, Inc., 1990.
[15] C. P. Robert, *Monte Carlo Methods*, Wiley Online Library, 2004.